Improving the performance of an actuator control scheme during saturation

Chang How Lo, Hyo-Sang Shin, Antonios Tsourdos, and Seung-Hwan Kim

Abstract This paper first introduces a new control scheme for a four fin missile actuation system. Exiting missile autopilot systems generally compute aileron, elevation, and rudder commands since these three variables dominantly influence the roll, pitch, and yaw motion of the vehicle. These commands are distributed to four fin deflection commands and fin controller actuates the fins to track the defection command. The performance of such control schemes can be significantly degraded when fin actuators are saturated due to certain physical constraints, such as voltage, current, or slew rate limit. This paper analytically proves that the proposed control scheme mitigates this problem, so it outperforms the conventional control scheme in the tracking performance if an actuator is saturated. Without any actuator saturation, the performance of the proposed scheme is also proved to be equivalent to that of a conventional actuator scheme. Numerical simulations verify the superiority of the proposed scheme and the theoretical analysis.

1 Introduction

The performance of the actuation system plays a decisive role in determining the performance of the flight control system, especially for a highly manoeuvrable air vehicles [8]. The vehicles are generally controlled by fins of which defection produces aerodynamic force. However, in classical autopilot design, the autopilot produces virtual roll, pitch and yaw moment demands [2] instead of physical fin deflection commands. These moment demands are then 'mixed'or allocated by an control allocation algorithm to generate individual actuator commands. The actuator com-

Chang How Lo, Hyo-Sang Shin, and Antonios Tsourdos
Cranfield University, College Road, Cranfield, Bedfordshire, MK43 0AL, United Kingdom, e-mail: c.lo@cranfield.ac.uk, h.shin@cranfield.ac.uk, a.tsourdos@cranfield.ac.uk

Seung-Hwan Kim,
ADD (Agency for Defense Development), Daejeon, Korea, e-mail: shadd@hanmail.net

mands will typically be tracked by their individual actuator controllers. Common problems faced in the actuators are that they may be saturated due to their physical constraints such as voltage, current, or slew rate limit. These problems can result in the significant performance degradation of the flight control system, or worse still, destablize the entire system.

Many approaches have been proposed to tackle this problem. One way is to treat this as a control allocation problem, and methods such as redistributed pesudo inverse [10], dynamic control allocation [5], and direct allocation [4] have been devised to optimally handle these actuator constraints. However, many control allocation methods do not track the actuator's actual performance, and thus possible deviations from the desired autopilot virtual commands can happen whenever there are unexpected degradations in the physical actuator due to faults, or disturbances.

In the design aspect, numerous control methodologies have been researched on in designing control schemes to handle actuator saturations and constraints with considerations on the stability, domain of attraction, and performance of actuation system. Extensive reviews and design methodologies of them can be found in Ref. [1] and Ref. [6]. In a typical conventional actuator scheme, each actuator has a dedicated controller to track its assigned command from a outer control loop. Practical implementations of such schemes are commonly found; an example is Ref. [11].

However, many of these methodologies aim at the design of a single actuator, and not as an actuation system. This may not fully exploit the analytical redundancies found in many systems to improve on the performance, or enhance its robustness to faults.

In our previous study [8], a new alternative actuator control scheme for a four tail fin controlled missile is proposed to alleviate the performance degradation results from actuator saturation. To utilize the analytically redundant actuator, the proposed scheme regulates the error in the virtual moment space rather than the physical fin deflection space. This alternative approach contrasts with ideas from Ref. [12], where linear in-line filters are used to exploit the actuator redundancy space to alleviate input rate and magnitude saturations.

This paper extends on our previous work in Ref. [8] to theoretically analyse the performance of the proposed actuator control system, which presented simulation results without formal proof. The main aim of this analysis is to analytically show that the proposed scheme outperforms the conventional actuator control scheme under actuator saturation. The performance index for the analysis is defined as the magnitude of the actuator tracking error, since the smaller the tracking error is, the better the performance is. From the analysis, in unsaturated operation region, it is proved that the performance of the proposed scheme is equivalent to that of a conventional scheme. The superior performance of the proposed scheme is also proved when one actuator is saturated. Simulation results verifying the analysis is then shown.

The organization of the rest of the paper is as follows. A description of the conventional and proposed control schemes are presented in Section 2. The main results of the paper are presented in Section 3, where the two control schemes are compared

analytically. In Section 4, the simulation setup is described, and simulation results verifying the analysis are shown. Finally, the paper is concluded in Section 5.

2 Description of Control Scheme

2.1 Conventional Control Scheme

Figure 1 shows a conventional actuator control architecture for a four tail fin controlled missile. A classical autopilot outputs virtual command $\delta_{\mathbf{mc}}$ in the roll, pitch and yaw moment space to the actuators. These commands are then allocated or mixed to individual actuator's controller for tracking by their local controller. The response achieved from actuator controllers in the moment space can be found by deallocating the individual actuator response as a measure of the control performance.

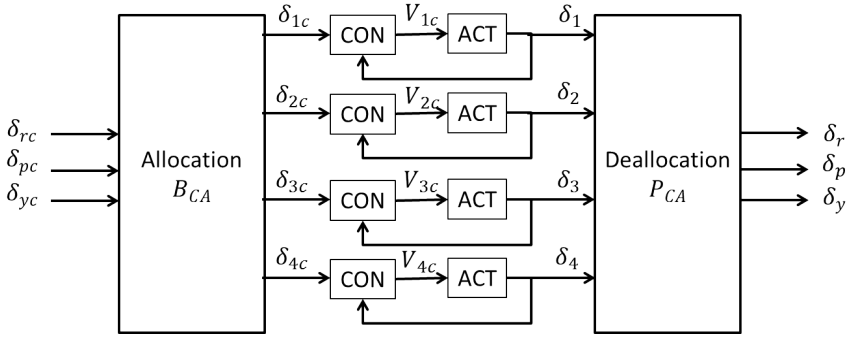

Fig. 1 Conventional Actuator Control Architecture

The closed loop transfer function for the conventional actuator control scheme for the autopilot demands is

$$\begin{aligned}\mathbf{G_o}(\mathbf{s}) &= \frac{\delta_{\mathbf{m}}(\mathbf{s})}{\delta_{\mathbf{mc}}(\mathbf{s})} \\ &= \mathbf{P_{ca}}\left(\frac{\mathbf{K}\mathbf{K_s}\mathbf{G}}{\mathbf{I}+\mathbf{K}\mathbf{K_s}\mathbf{G}}\right)\mathbf{B_{ca}} \end{aligned} \tag{1}$$

where $\delta_{\mathbf{mc}} = \begin{bmatrix}\delta_{rc} & \delta_{pc} & \delta_{yc}\end{bmatrix}^T$ is the virtual control demand from the autopilot, $\delta_{\mathbf{m}} = \begin{bmatrix}\delta_r & \delta_p & \delta_y\end{bmatrix}^T$ is the resultant response from the actuators in the virtual space, $\mathbf{K} = diag(K_i)$ is the actuator controller. The i^{th} actuator is described by two terms: a linear actuator model G_i, which is preceded by a physical voltage constraint K_{is}. The four actuators can be combined mathmatically as $\mathbf{G} = diag(G_i)$ and $\mathbf{K_s} = diag(K_{is})$. K_{is}

is the standard saturation function to describe the physical voltage input constraint, V_c. In frequency domain, the nonlinear saturation function can be represented as

$$K_{is} = 1, \qquad |V_c| \leq V_{max} \tag{2}$$

$$0 < K_{is} < 1, \qquad |V_c| > V_{max} \tag{3}$$

It is assumed there is no unstable pole zero cancellation in the system. For a four tail fin missile under consideration here, the control allocation matrix is

$$\begin{gathered} \delta = \mathbf{B_{ca}}\,\delta_{\mathbf{m}} \\ \begin{bmatrix} \delta_1 \\ \delta_2 \\ \delta_3 \\ \delta_4 \end{bmatrix} = \begin{bmatrix} 1 & 1 & -1 \\ 1 & 1 & 1 \\ 1 & -1 & 1 \\ 1 & -1 & -1 \end{bmatrix} \begin{bmatrix} \delta_r \\ \delta_p \\ \delta_y \end{bmatrix} \end{gathered} \tag{4}$$

and the deallocation matrix $\mathbf{P_{ca}}$ being

$$\mathbf{P_{ca}} = \frac{1}{4} \begin{bmatrix} 1 & 1 & 1 & 1 \\ 1 & 1 & -1 & -1 \\ -1 & 1 & 1 & -1 \end{bmatrix} \tag{5}$$

with

$$\mathbf{P_{ca}B_{ca}} = \mathbf{I} \tag{6}$$

or $\mathbf{P_{ca}}$ being the pseudo inverse solution of $\mathbf{B_{ca}}$. The control allocation matrix is obtained by considering the resultant torque generated by each actuator's position from the aerodynamics point of view.

2.2 Proposed Control Scheme

Figure 2 shows the control scheme first proposed in our previous study [8]. Here, the actuator control scheme regulates the tracking error in the virtual moment space space before control allocation. This contrasts with the conventional control scheme regulating the physical tracking error of each individual actuator. The closed loop transfer function of the proposed scheme can be derived as

$$\mathbf{G_n}(\mathbf{s}) = \frac{\mathbf{K\,P_{ca}\,K_s\,G\,B_{ca}}}{\mathbf{I + K\,P_{ca}\,K_s\,G\,B_{ca}}} \tag{7}$$

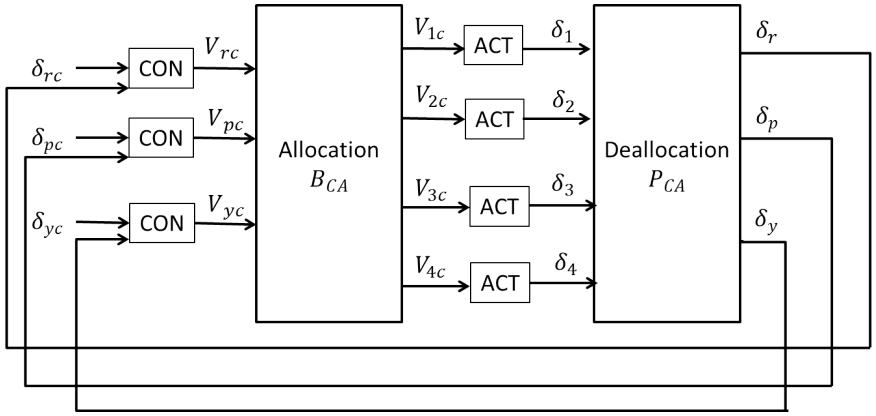

Fig. 2 Proposed Actuator Control Architecture

3 Comparison of Control Schemes

The comparison of the two control schemes is divided into two cases: linear (non-saturating) case, and when one actuator is saturated.

3.1 Non saturation case

Replacing K_{is} with unity gain in Equations 1 and 7, and assuming the actuators and their controllers are similar $G_i = G$ and $K_i = K$, it can be verified that both control schemes can be reduced to the following linear transfer function:

$$\frac{\boldsymbol{\delta}_{\mathbf{m}}(\mathbf{s})}{\boldsymbol{\delta}_{\mathbf{mc}}(\mathbf{s})} = \frac{GK}{GK+1}\begin{bmatrix} 1 & 0 & 0 \\ 0 & 1 & 0 \\ 0 & 0 & 1 \end{bmatrix} \tag{8}$$

The significance of this case is to show the two control schemes are equivalent during nominal operation, and proof that the improvement in performance of the proposed scheme shown later is not due to increase in gain. In practice, this may reduce the amount of design analysis needed to convert from the proposed scheme for any existing actuator scheme.

3.2 One actuator saturation case

Next, the analysis is extended to the case when one actuator is saturated during operation. First, assume Actuator Number 4 is saturated. This can be represented by

$$\mathbf{K_s} = \begin{bmatrix} 1 & 0 & 0 & 0 \\ 0 & 1 & 0 & 0 \\ 0 & 0 & 1 & 0 \\ 0 & 0 & 0 & K_{4s} \end{bmatrix} \tag{9}$$

where $K_{4s} < 1$. Substituting Equation 9 into Equation 7 for the proposed scheme, and rearranging with Equation 5 reveals

$$\begin{aligned} \delta_r &= \left(\frac{GK}{GK+1}\right)\delta_{rc} \\ &\quad + \left(\frac{K_{4s}-1}{K\left(G+3GK_{4s}\right)+4}\right)\begin{bmatrix} 1 \\ -1 \\ -1 \end{bmatrix}^T \begin{bmatrix} \delta_{rc} \\ \delta_{pc} \\ \delta_{yc} \end{bmatrix} \\ &= \left(\frac{GK}{GK+1}\right)\delta_{rc} \\ &\quad + \frac{1}{4}\left(\frac{K_{4s}-1}{K\left(G+3GK_{4s}\right)+4}\right)\delta_{4c} \end{aligned} \tag{10}$$

$$\begin{aligned} \delta_p &= \left(\frac{GK}{GK+1}\right)\delta_{pc} \\ &\quad + \left(\frac{K_{4s}-1}{K\left(G+3GK_{4s}\right)+4}\right)\begin{bmatrix} -1 \\ 1 \\ 1 \end{bmatrix}^T \begin{bmatrix} \delta_{rc} \\ \delta_{pc} \\ \delta_{yc} \end{bmatrix} \\ &= \left(\frac{GK}{GK+1}\right)\delta_{pc} \\ &\quad - \frac{1}{4}\left(\frac{K_{4s}-1}{K\left(G+3GK_{4s}\right)+4}\right)\delta_{4c} \end{aligned} \tag{11}$$

$$\begin{aligned} \delta_y &= \left(\frac{GK}{GK+1}\right)\delta_{yc} \\ &\quad + \left(\frac{K_{4s}-1}{K\left(G+3GK_{4s}\right)+4}\right)\begin{bmatrix} -1 \\ 1 \\ 1 \end{bmatrix}^T \begin{bmatrix} \delta_{rc} \\ \delta_{pc} \\ \delta_{yc} \end{bmatrix} \\ &= \left(\frac{GK}{GK+1}\right)\delta_{yc} \\ &\quad - \frac{1}{4}\left(\frac{K_{4s}-1}{K\left(G+3GK_{4s}\right)+4}\right)\delta_{4c} \end{aligned} \tag{12}$$

Equations 10 to 12 show the effect of actuator saturation. The first term on the right hand side of these equations is the nominal unsaturated performance of the actuator, while the second term is the additional dynamics introduced by the saturated

actuator. For the conventional scheme, similar relationships can be obtained by manipulating Equation 1 in the same manner to obtain Equations 13 to 15:

$$\begin{aligned}\delta_r &= \left(\frac{GK}{GK+1}\right)\delta_{rc} \\ &\quad + \left(\frac{K_{4s}-1}{4GKK_{4s}+4}\right)\begin{bmatrix}1\\-1\\-1\end{bmatrix}^T\begin{bmatrix}\delta_{rc}\\\delta_{pc}\\\delta_{yc}\end{bmatrix} \\ &= \left(\frac{GK}{GK+1}\right)\delta_{rc} \\ &\quad + \frac{1}{4}\left(\frac{K_{4s}-1}{4GKK_{4s}+4}\right)\delta_{4c}\end{aligned} \tag{13}$$

$$\begin{aligned}\delta_p &= \left(\frac{GK}{GK+1}\right)\delta_{pc} \\ &\quad + \left(\frac{K_{4s}-1}{4GKK_{4s}+4}\right)\begin{bmatrix}-1\\1\\1\end{bmatrix}^T\begin{bmatrix}\delta_{rc}\\\delta_{pc}\\\delta_{yc}\end{bmatrix} \\ &= \left(\frac{GK}{GK+1}\right)\delta_{pc} \\ &\quad - \frac{1}{4}\left(\frac{K_{4s}-1}{4GKK_{4s}+4}\right)\delta_{4c}\end{aligned} \tag{14}$$

$$\begin{aligned}\delta_y &= \left(\frac{GK}{GK+1}\right)\delta_{yc} \\ &\quad + \left(\frac{K_{4s}-1}{4GKK_{4s}+4}\right)\begin{bmatrix}-1\\1\\1\end{bmatrix}^T\begin{bmatrix}\delta_{rc}\\\delta_{pc}\\\delta_{yc}\end{bmatrix} \\ &= \left(\frac{GK}{GK+1}\right)\delta_{yc} \\ &\quad - \frac{1}{4}\left(\frac{K_{4s}-1}{4GKK_{4s}+4}\right)\delta_{4c}\end{aligned} \tag{15}$$

Similarly, the effects of actuator 4's saturation can be accounted for the conventional actuator scheme. The second term on the right hand side of Equations 13 to 15 is the detrimental contribution by the saturation.

Comparing between the proposed and conventional schemes, it can be seen the numerator of the saturation dynamics for both schemes are the same at $(K_{4s}-1)$ from Equations 10 to 15. Now, comparing the denominator of conventional and proposed scheme, it can be seen that

$$(4GKK_{4s}+4) < (GK+3GKK_{4s}+4) \tag{16}$$

by noting that $K_{4s} < 1$ during actuator saturation. This implies the magnitude of the effect caused by the saturation term for the conventional scheme will be bigger than the proposed scheme. The alleviation in actuator saturation in the proposed scheme in this case is due to the availability of actuator redundancy, which enables the controller to increase the commands of the other non-saturated actuators.

The same results are obtained when saturations occur with other actuators in the control scheme. For the single actuator saturation case, the proposed control scheme's results in Equations 10 to 12 can be generalised to

$$\delta_{\mathbf{mc}} = \frac{GK}{GK+1}\left(\mathbf{I}+\mathbf{P_{ca}DB_{ca}}\right)\delta_{\mathbf{m}} \tag{17}$$

with the appropriate actuator being saturated, and the other K_{is} being equal to 1. For the proposed actuator scheme, $\mathbf{D}$ is defined as

$$\mathbf{D} = diag\left[4\left(\frac{K_{is}-1}{KG+3GKK_{is}+4}\right)\right] \tag{18}$$

Similarly, the corresponding single actuator saturation case using conventional actuator control scheme's results, described in Equations 13 to 15, can be generalised to Equation 17, with $\mathbf{D}$ defined as

$$\mathbf{D} = diag\left[4\left(\frac{K_{is}-1}{4GKK_{is}+4}\right)\right] \tag{19}$$

The generalizations here assumes the structure of $\mathbf{B_{ca}}$ and $\mathbf{P_{ca}}$, and their relationship described in Equations 4 to 6. Overall, one can see that the proposed scheme is superior to the conventional scheme, as the magnitude of $\mathbf{D}$ in Equation 18 for the proposed scheme is smaller than the magnitude of $\mathbf{D}$ in Equation 19 for the conventional scheme. Next, simulations results are presented.

4 Simulation

4.1 Simulation Model

The actuator plant used in the simulation is described in [8], which is shown in Figure 3. The plant is a typical DC motor with gearing, and explained in Ref. [3]. The parameters used in are detailed in Table 1.

A cascaded two loop controller shown in Figure 4 is used to provide good control performance of the actuator plant from Ref. [8]. The control law is

Table 1 Actuator plant parameters used in the simulation

Parameters	Values	Parameters	Values
K_T	0.303125	K_B	$5.7333x10^{-4}$
L	0.35×10^{-3}	H	0
R	0.933	V_{lim}	28
J	8.5354×10^{-7}	N	274
B	2.0835×10^{-6}		

$$V_c(t) = K_p\left(\delta_c(t) - \delta(t)\right) - K_d\left(\dot{\delta}(t)\right) \tag{20}$$

where δ_{ci} is the commanded deflection angle, and $K_p = 6$ and $K_d = 0.02$ are gains for the control law. The reference command used in this simulation is a sinusoidal input at 0.3 rad/sec as input virtual commands for all 3 virtual demands. This continuously changing reference input allows for visualisation of the differences between the two control schemes.

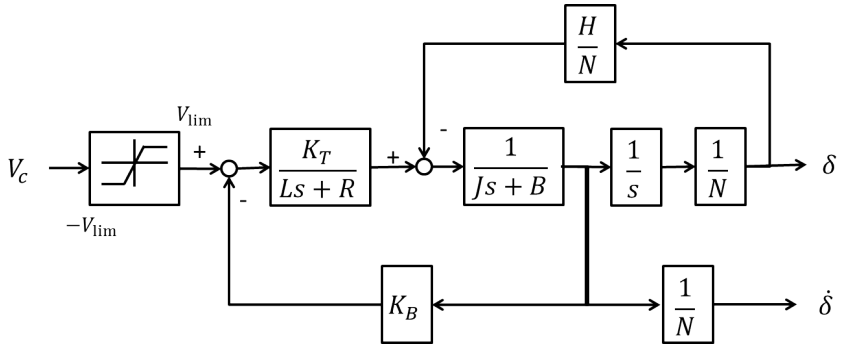

Fig. 3 Actuator plant model used in the simulation

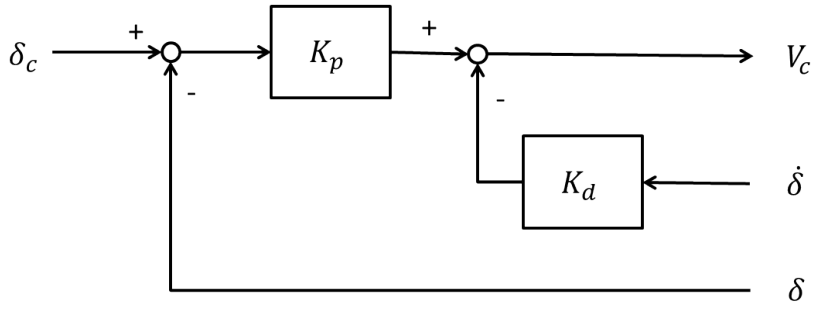

Fig. 4 Controller used for controlling the actuator plant used in the simulation

4.2 Simulation Results

The unsaturated simulation results are first shown in Figures 5 and 6. The two control schemes perform exactly the same as expected from theoretical analysis presented earlier.

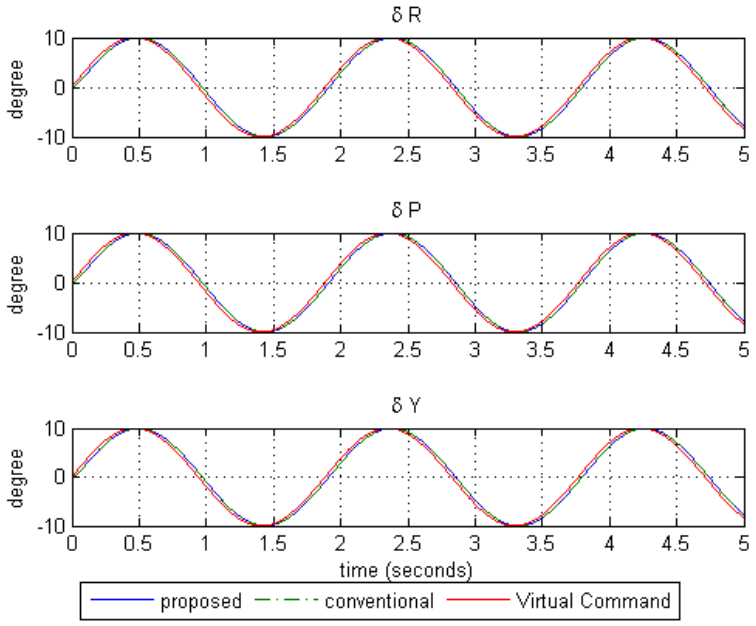

Fig. 5 Simulation results showing the 2 control schemes having exact responses when there is no actuator saturation events. The blue line is the proposed scheme, green dotted line is the conventional scheme, and red line is the virtual command

To simulate the effect of actuator saturation, the maximum voltage input level for Actuator Number 2 is reduced by 90 percent of its original value. This can also be thought of the actuator having a fault to reduce its effectiveness.

Figure 7 shows the simulation results with Actuator Number 2 voltage range reduced. The proposed scheme is able to track the virtual demand relatively well for all three virtual demands. In contrast, the conventional scheme shown with green dotted line exhibits poor tracking consistent across the three virtual demands. Figure 8 shows the individual actuator responses for the same simulation. It can be seen the proposed scheme is able to exploit the available actuator capability when actuator 2 is saturated to improve the performance over the conventional scheme. This also implies the need for the remaining healthy unsaturated actuators to have remaining actuator margins in physical constraints for the proposed scheme to exploit.

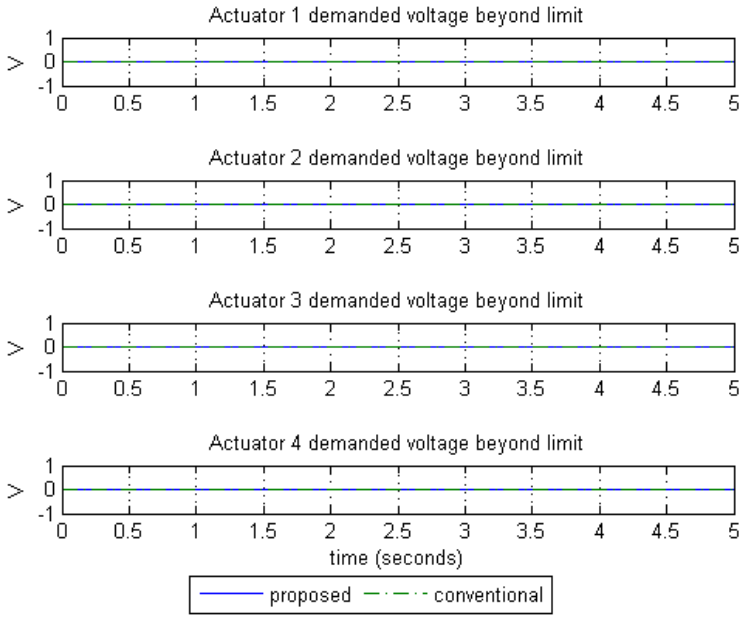

Fig. 6 Simulation plots showing no saturation results showing the 2 control schemes having exact responses when there is no actuator saturation events. The blue line is the proposed scheme, green dotted line is the conventional scheme, and red line is the virtual command

5 Conclusion

Analytical analysis of a proposed actuator control scheme over conventional control scheme is presented. By directly regulating tracking error in the moment space, the change in the control variables over conventional actuator control schemes improves the tracking performance during actuator saturation when there is available actuator redundancy available. The proposed scheme is shown to be superior in performance when one actuator is saturated with smaller magnitude in the error dynamics. This is due to its ability to utilize the available redundancy to reduce the performance degradation. Simulations verified the theoretical analysis.

References

1. D. Bernstein and A. Michel, “A chronological bibliography on saturating actuators,” *International Journal of robust and nonlinear control*, vol. 5, no. 5, pp. 375–380, 1995.
2. J. Blakelock, *Automatic control of aircraft and missiles*. Wiley-Interscience, 1991.
3. R. Dorf and R. Bishop, *Modern control systemss*. Prentice Hall, 2001.

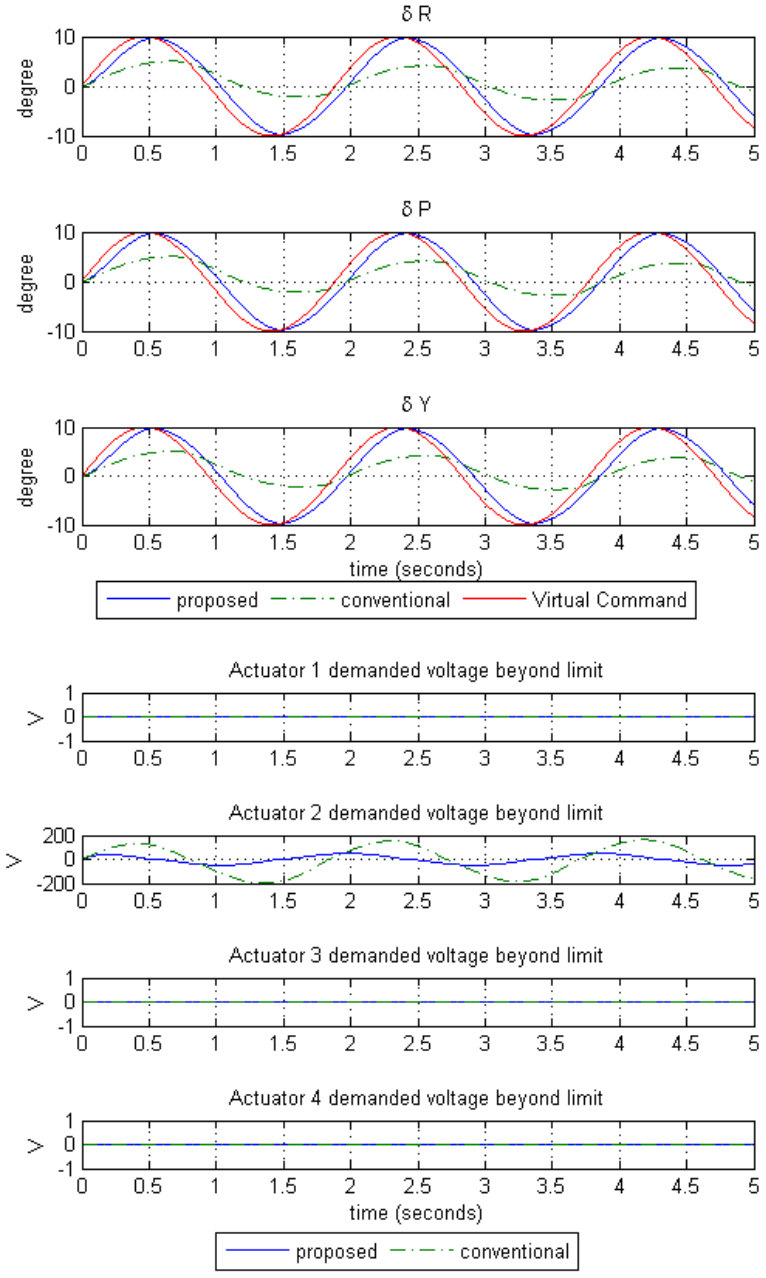

Fig. 7 Simulation results for 1 actuator saturation case. The blue line is the proposed scheme, green dotted line is the conventional scheme, and red line is the virtual command

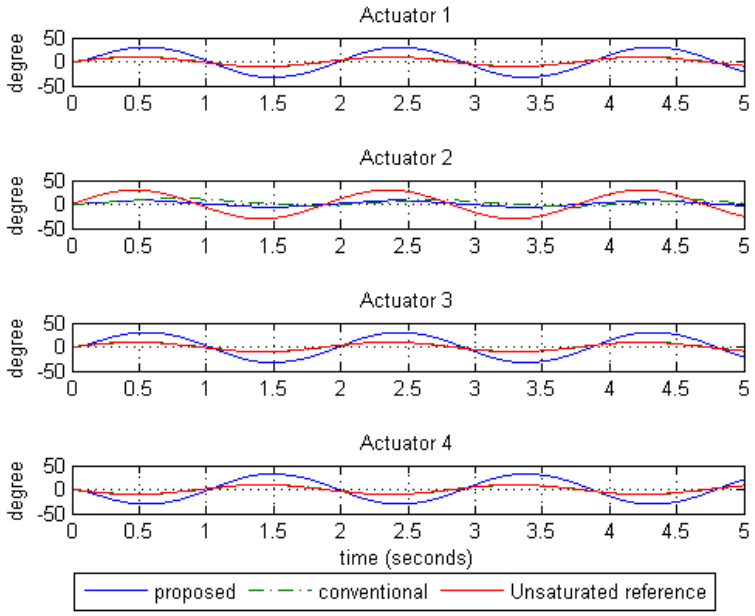

Fig. 8 Individual actuator responses for 1 actuator saturation case. The blue line is the proposed scheme, and green dotted line is the conventional scheme. The red line shows the unsaturated reference signal from previous simulation in comparison.

4. W. Durham, "Constrained control allocation," *Journal of Guidance, control, and Dynamics*, vol. 16, no. 4, pp. 717–725, 1993.
5. O. Harkegard, "Dynamic control allocation using constrained quadratic programming," *Journal of Guidance Control and Dynamics*, vol. 27, no. 6, pp. 1028–1034, 2004.
6. T. Hu, Z. Lin, and B. Chen, "An analysis and design method for linear systems subject to actuator saturation and disturbance," *Automatica*, vol. 38, no. 2, pp. 351–359, 2002.
7. T. Johansen, "Optimizing nonlinear control allocation," in *Decision and Control, 2004. CDC. 43rd IEEE Conference on*, vol. 4. IEEE, 2004, pp. 3435–3440.
8. S. Kim, Y. Lee, and M. Tahk, "New structure for an aerodynamic fin control system for tail fin-controlled stt missiles," *Journal of Aerospace Engineering*, vol. 24, no. 4, 2011.
9. Y. Luo, A. Serrani, S. Yurkovich, D. Doman, and M. Oppenheimer, "Dynamic control allocation with asymptotic tracking of time-varying control input commands," in *American Control Conference, 2005. Proceedings of the 2005*. IEEE, 2005, pp. 2098–2103.
10. M. Oppenheimer, D. Doman, and M. Bolender, "Control allocation for over-actuated systems," in *Control and Automation, 2006. MED'06. 14th Mediterranean Conference on*. IEEE, 2006, pp. 1–6.
11. L. Yount and J. Todd, "Flight control module with integrated spoiler actuator control electronics," May 13 2003, uS Patent 6,561,463.
12. L. Zaccarian, "Dynamic allocation for input redundant control systems," *Automatica*, vol. 45, no. 6, pp. 1431–1438, 2009.